Article

Not peer-reviewed version

Effects of Riparian Vegetation on the Evolution of an Experimental Meandering Channel Downstream a Scour Pit

Xiaolong Song *, Haijue Xu, Yuchuan Bai

Posted Date: 3 February 2023

doi: 10.20944/preprints202302.0064.v1

Keywords: Riparian vegetation; Experimental meandering channel; Scour pit; Downstream scroll bars; Inner-bank cutting; evolutionary spectral analysis

Article

Effects of Riparian Vegetation on the Evolution of an Experimental Meandering Channel Downstream a Scour Pit

Xiaolong Song [1,2,*], Haijue Xu [1,2] and Yuchuan Bai [1,2]

[1] State Key Laboratory of Hydraulic Engineering Simulation and Safety, Tianjin University, Tianjin, China;
[2] Institute for Sedimentation on River and Coastal Engineering, Tianjin University, Tianjin, China;
* Correspondence: xlsong@tju.edu.cn

Abstract: We conducted the meander evolution experiments incorporating the effects of riparian vegetation and the series of upper vortex flow disturbances induced by a scour pit simultaneously. Two employed nonlegume plants with salinity and alkalinity resistance, had uniform degrees of seedling normal growth and different lengths of root networks. Our results show that riparian vegetation in general can consolidate the single-thread channel planform without branching outward under the flooding flow conditions. Transverse point bars on inner banks were instead by downstream scroll bars in overall channel for long, unless the coupling of riparian vegetation and flood scour. Shallow-rooted plant was inadequate to resist the inner-bank cutting effect brought by the upper vortex flow. Deep-rooted plant can stabilize the bank-lines and thalweg significantly, but that was susceptible to locally low vegetation coverage. Using evolutionary spectral analysis based on thalweg, we found streamwise high-frequency distribution of bed topography mainly concentrated downstream the bifurcation interface in unvegetated scenario when faced with a flood, shrank to the upper isolated turning interface in shallow-rooted scenario, and conversely stood out along the bare roots disturbed region in deep-rooted scenario. This experimental study expands a much wider understanding of vegetation effects in hydro-bio-geomorphological systems engineering.

Keywords: riparian vegetation; experimental meandering channel; scour pit; downstream scroll bars; inner-bank cutting; evolutionary spectral analysis

1. INTRODUCTION

The near-river biotic community, riparian vegetation, plays an important role in regulating the morphological development of a river, through physically bank strengthening (Crosato & Saleh, 2011; Gran & Paola, 2001; Parker et al., 2011; Song & Bai, 2015; Tal & Paola, 2007; van Dijk, Teske, et al., 2013) and biologically system energizing (Song et al., 2022; Zalewski, 2013, 2015). Mature riparian vegetation is able to promote the concentration of channel flow, the maintenance of meandering channel pattern, and the overall forward evolution in the systematic out-branching form induced by stochastic event processes (Song et al., 2022). While undeveloped and loosely distributed vegetation may lead to the delay of point-bar accretion following the outer bank retreat and result in the aggravation of multi-thread transitioning (Kyuka et al., 2021) within the smoothly and simply external bank-lines. Flood-induced plant uprooting also may gradually reduce the mechanical anchoring of roots and constitute a key component variable in this fully coupled eco-geomorphological system (Camporeale et al., 2013; Perona & Crouzy, 2018).

Some field observations confirmed the effects of vegetation establishment on various river morphology, including braided rivers (Gran et al., 2015), alternate bars (Serlet et al., 2018) and sinuous channels (Bywater-Reyes et al., 2018): newly formed deposits can be stabilized by deflecting

 doi:10.20944/preprints202302.0064.v1

the flow with the aid of root networks (Bywater-Reyes et al., 2018); bare soil can be protected by the vegetation cover and soil moisture content can be lowered via interception and evapotranspiration, thus to bring the pore water pressure down (Terwilliger, 1990); in some cases, increased infiltration rates during heavy rainfall (Simon & Collison, 2002) and additional weight on banks (Abernethy & Rutherfurd, 2000) owing to the presence of vegetation also can worsen river evolution. While, numerical models have been considering the effects of vegetation on river morphodynamic processes in highly simplified ways (Bertoldi et al., 2014; Jang & Shimizu, 2007; Vargas-Luna et al., 2016); multiple interactions are present during the abiotic-biotic processes (van Dijk, Teske, et al., 2013), such as seed dispersal, recruitment, vegetation growth, and, sediment substrate, uprooting, etc., these factors are very difficult to be controlled quantitatively. Experimental method is still most widely accepted to investigate the eco-geomorphological behaviors in river.

The response of river landscapes to climate and tectonic changes often gives shape to quasi-vertical knickpoints (waterfalls) (Scheingross & Lamb, 2017). In fluid dynamics, vortex shedding process has been well understood when water drills vertically (or flows past a bluff body) at certain velocities, in which vortices are created at the back of the scour pit (or body) and detach periodically from either side of the pit forming a Von Kármán vortex street. In nature, waterfalls can significantly determine the distribution of lotic organisms along the rivers, cause species differences above and below waterfalls and contribute to the flourish of diverse communities of terrestrial species along with a microclimate developing in their immediate vicinity characterized by cooler temperatures and higher humidity than the surrounding region (Björk et al., 2009). But little work has been done on integrated evolution of upper waterfall plunge pool and lower river (Scheingross & Lamb, 2017), in particular, the river morphology variations incorporating the upper dynamic vortex flow disturbances and the validity of the above confirmed regulating ability of riparian vegetation in meander evolutions.

Here, we focus on experimental meandering channels driven by an upper vortex flow with the development of a scour pit from a minitype waterfall, to investigate how different bank vegetating schemes affect the river evolution. A weak, sine-generated meandering channel and two kinds of nonlegume, saline-alkali resistant plants were employed. The channel planform and bed topography changes before and after a flood were then innovatively analyzed in three different scenarios (including the unvegetated case), especially, some changes in river morphology demonstrated that the bank pull or bar push concept that describes the scroll-bar development on the inner banks of a meandering channel (van de Lageweg et al., 2014) may not apply.

2. EXPERIMENTAL DESIGN

2.1. Flume setup

Experiments were conducted in a 3.60-m long, 1.70-m wide and 0.20-m high self-developed rectangular river-simulator flume, located at the Institute for Sedimentation on River and Coastal Engineering, Tianjin University in China (Figure 1). The meander-evolution region of flume was initially filled with an 8-cm thick layer of cohesionless fine sediment; Figure 2 shows the grain size distribution curve (median grain size D_{50} = 0.1mm, geometrical standard deviation $\sigma_g = (D_{84}/D_{16})^{1/2}$ = 1.7). A 5-cm width fixed inlet channel was connected to the shaping initial single-thread channel with approximately a width of 15 cm, depth of 2.5 cm, slope of 1.5%, streamwise wavelength of 0.52 m, maximum deflection angle of 35° and ratio of bending radius to width of 3.0; bed level difference at the junction of the two types of channels was set to be 1 cm in each experiment for generating a scour pit and the corresponding dynamic vortex flow; a 0.50-m long movable straight segment was located between the fixed inlet channel and sine-generated meandering channel to smooth the incoming flow and sediment. The channel excavation followed Song et al. (2016)'s method.

Preprints.org (www.preprints.org) | NOT PEER-REVIEWED | Posted: 3 February 2023 doi:10.20944/preprints202302.0064.v1

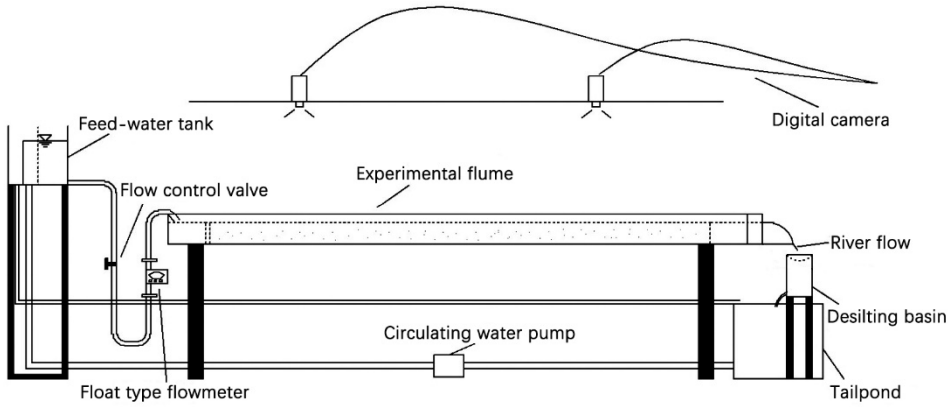

(a) Side-view schematic diagram of experimental environment

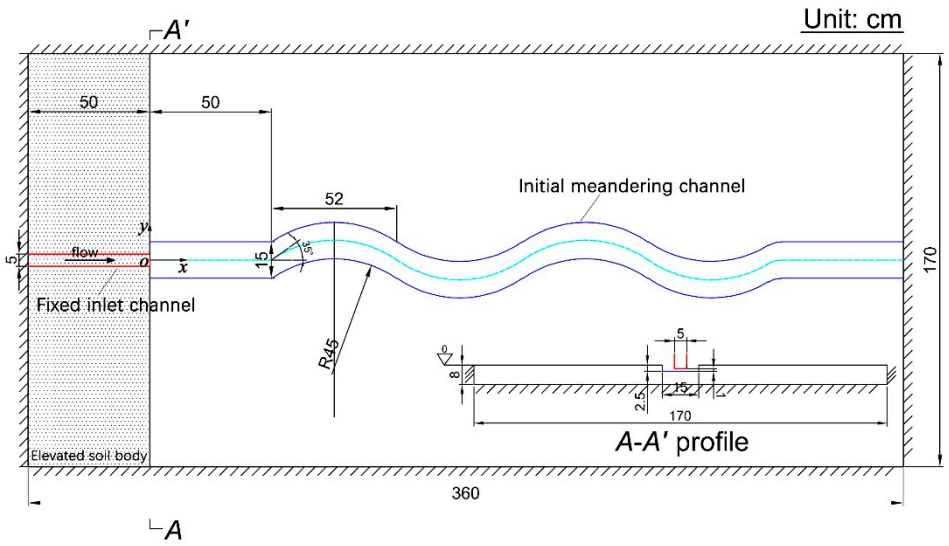

(b) Plan-view schematic diagram of flume and entry profile

Figure 1. Experimental facility setup.

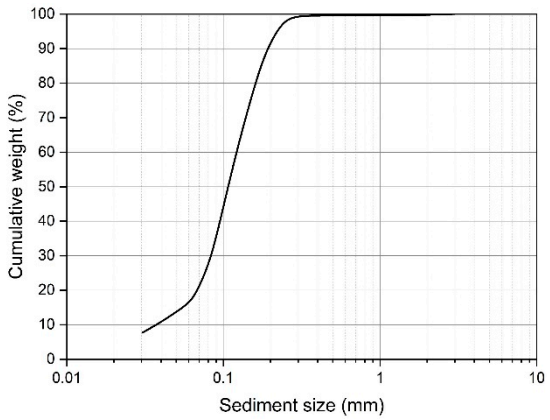

Figure 2. Grain-size distribution of sediment.

The upstream boundary of the movable bed region was soil wall, and the other boundaries were iron plates. A tailpond and a desilting basin was arranged at the flume outlet for water storing and sediment retaining, respectively. The water was transported to the upper feed-water tank driven by water pump and then flowed into the channels through a buckled pipe. The flow discharge was

 doi:10.20944/preprints202302.0064.v1

controlled by a valve, and the excess water from the pump could be directly diverted into the tailpond through the overflow pipe, which generally formed a closed self-circulation system of water (Yang et al., 2018).

2.2. Hydraulic and plant conditions, and data acquisition

Three experiments were performed that differed in riparian vegetation species and vegetated-bank strength, including cases of no vegetation (Run-a), non-uniformly grown deep-rooted Festuca elata (Run-b) and shallow-rooted Lolium perenne (Run-c). These two grasses have strong adaptation to the saline environment, but higher concentration of the salts delayed the preliminary seed germination time and inhibited the various degrees of seedling normal growth (Lu et al., 2002) under the same conditions of sowing density herein. The adopted discharge hydrograph consists of initial constant phase-1, middle increasing phase-2, and later decreasing phase-3 (Figure 3). After every 5 hours of running at the transition moments of different phases, the pump was stopped and the topography was measured using a laser range finder (every 5 cm longitudinally and 1 cm transversely, with a precision of 1 mm). River channel configuration was monitored through the digital cameras and bank-lines were identified using a self-developed image recognition system after image distortion correction and coordinate transformation (Song et al., 2014).

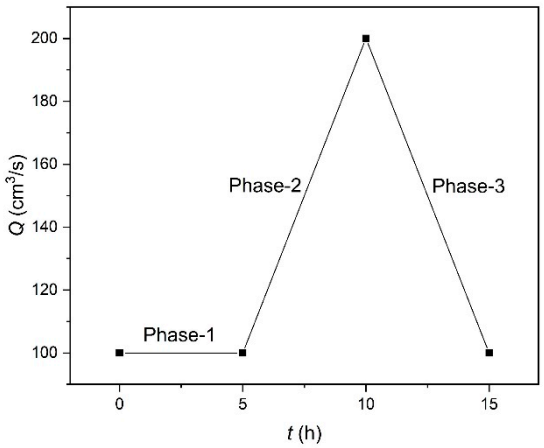

Figure 3. Experimental discharge hydrograph.

Plants cover the range distances of 30 cm away from the meandering river bank-lines in riparian zones. Seedlings germinated after about 2 days and experiments were conducted after 5 days of germination. The variations of indoor temperature and humidity during the vegetated experiments were recorded at a rate of 15 min; Table 1 shows the representative statistics.

Table 1. Ambient temperature and humidity during the vegetated experiment processes.

Run	Temperature (°C)		Humidity (%)	
	Mean	SD	Mean	SD
Run-b	19.3	2.4	80.1	6.2
Run-c	24.6	1.2	81.5	5.2

 doi:10.20944/preprints202302.0064.v1

3. RESULTS AND ANALYSIS

3.1. Channel planform changes

Experiments evaluating different effects of riparian vegetation showed different phased evolution of channel planform changes (Figures 4, 5 and 6). In the unvegetated scenario, channel migration was undeveloped in the downstream reach, active spiral erosion occurred along the outer-bank sides of upper and middle reaches with the formation of braided swales in phase-1 (Figure 4b). With the increasing of discharge, a dendric pattern of outer bank splay occurred on the floodplain (x=1.0~1.2m) to act as the incipient outward-branching channels (Song et al., 2022) and a series of downstream scrolled bars developed gradually instead of obvious points bars on the inner banks of bends in phase-2 (Figure 4c). In phase-3, the main channel continued to be deepened and its sinuosity was raised by the decreasing discharge (Figure 4a); the final outer bank inundation zone and downstream braided-scrolled bars were observed around the bifurcation interface of channel (Figure 4e).

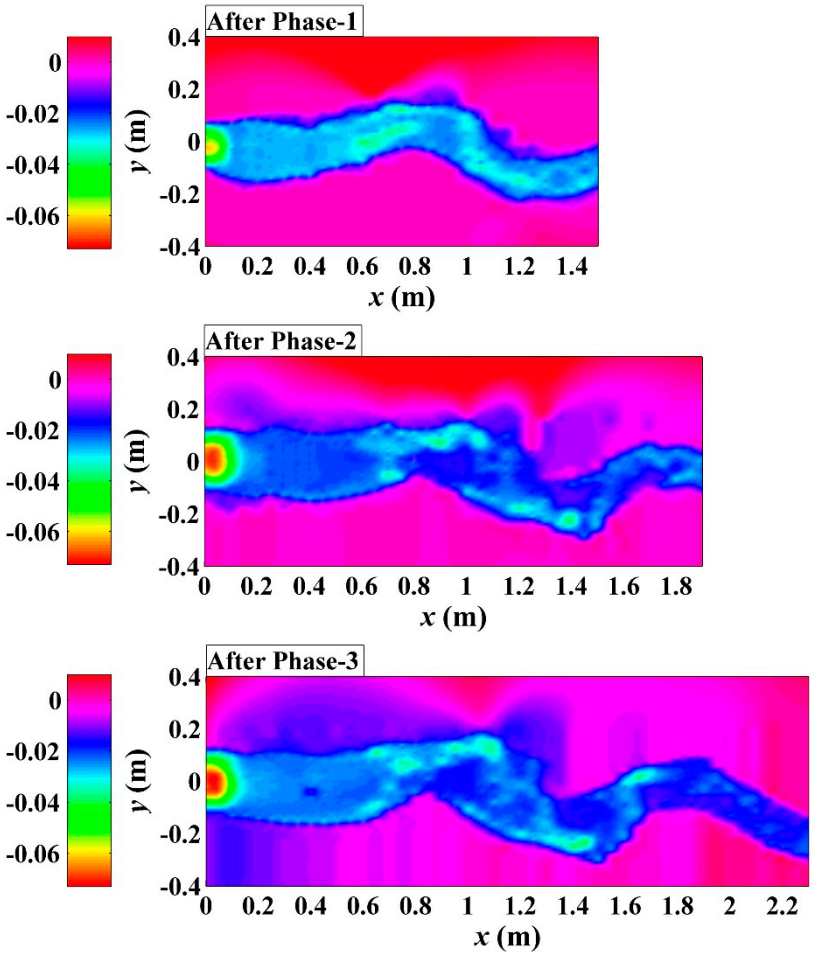

(a) Significant changes of DEMs (unit: m)

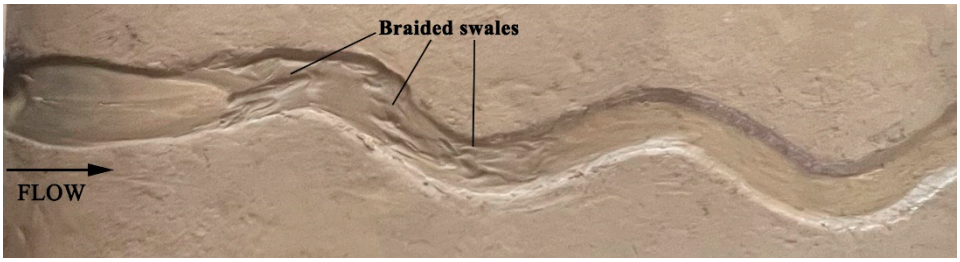

(b) Channel morphology after phase-1

 doi:10.20944/preprints202302.0064.v1

(c) Outer bank splay at the upstream bend (x=1.0~1.2m) in phase-2

(d) Downstream scrollbar morphology in phase-2

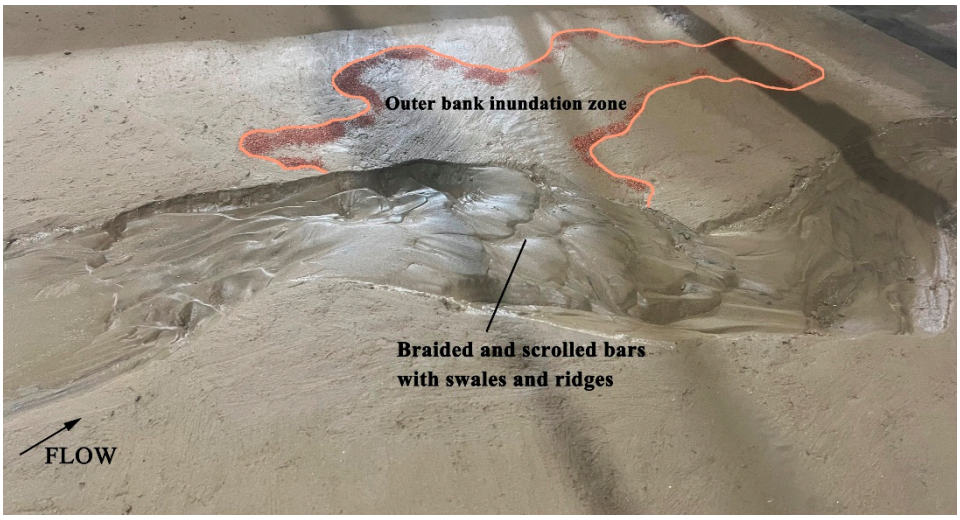

(e) Final floodplain morphology after phase-3

Figure 4. Phased evolutions of the unvegetated scenario (Run-a).

In the Festuca-elata vegetation scenario, bank erosion was inhibited with the increasing of bank strength, slight changes of channel planform were observed (Figure 5a). In phase-1, isolated spiral swales occurred along the outer bank of upstream bends instead of continuous braided swales, due to the flow disturbances of scoured bare plant roots (Figure 5b); downstream scrolled bars formed in the overall main flow channel (Figure 5c), still not yielding to point-bar patterns. After three days of compelled pump repairment and a frenzy of plant growth (to be lodging) during the break-in period, in phase-2, both bank strength and channel bed resistance were greatly enhanced, transverse scrolled bars (point bars) with ridges and swales appeared on the inner banks of bends clearly, driven by the

 doi:10.20944/preprints202302.0064.v1

increasing discharge (Figure 5d). Later, sinuosity and width-depth ratio of the main channel were little affected by the falling of discharge in phase-3 (Figure 5e).

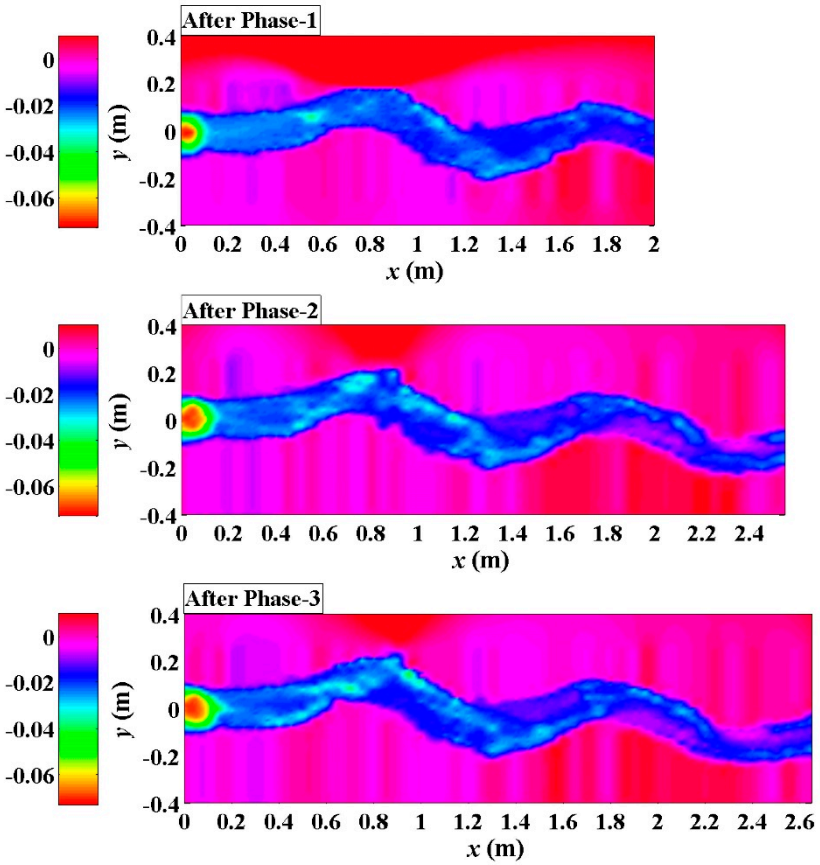

(a) Significant changes of DEMs (unit: m)

(b) Upper bends morphologies after phase-1

(c) Downstream scrollbar morphology after phase-1

 doi:10.20944/preprints202302.0064.v1

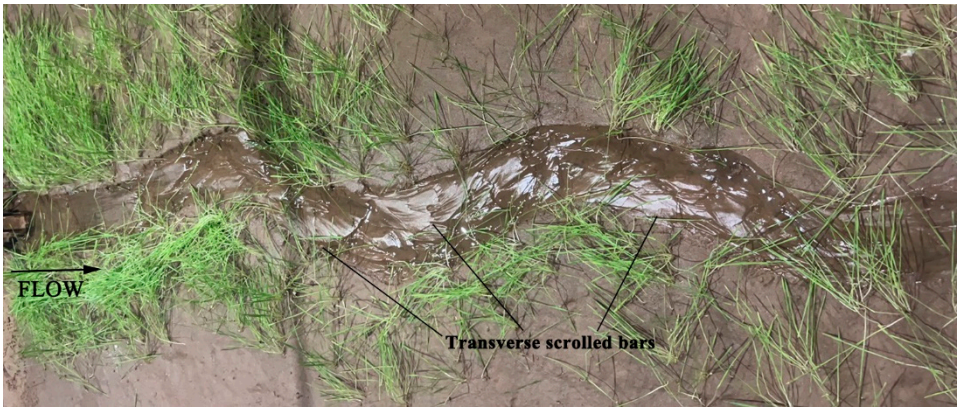

(d) Transverse scrollbar morphology in phase-2

(e) Transverse scrollbar morphology in phase-3

Figure 5. Phased evolutions of the Festuca-elata vegetation scenario (Run-b).

In the Lolium-perenne vegetation scenario, the introverted branching pattern (Song et al., 2022) was still dominated in the evolution process of channel planform (Figure 6a), similar to the Festuca-elata vegetation scenario. Braided and downstream scrolled bars were observed after phase-1 (Figure 6b), due to the limitation of lateral channel migration imposed by bank vegetating and the non-disturbance of the shallow roots to flow. In phase-2, the increasing discharge resulted in the large-scale spiral swales mixing up with braded bars in the upstream bend (Figure 6c) and the formation of transverse scrolled bars along the inner-bank sides of overall meandering channel (Figure 6d). In phase-3, the point bars in the lower reach got support from the decreasing discharge for further development and growth (may well be stemming from the local sparse vegetation cover), a clear gradient developed along the interface between point bars and the main flow channel, and a large-scale spiral swale occurred between such adjacent bars (Figure 6e).

The phased routes of longitudinal synchronized bank-line and thalweg migrations of main-channel in each scenario are compared as shown in Figure 7. In the unvegetated scenario (Figure 7a), upstream straight segment (x<0.4m) was widened and narrowed with the rising and falling of discharge. Bank cutting and erosion continuously occurred at the inner bank (0.4m<x<0.8m) and outer bank (1.0m<x<1.2m) of the No.1 main channel bend respectively and pushed the bank-lines to gradually move downstream and outward. While the inner bank was not cut any more after entering the No. 2 main channel bend (x>1.3m), the main flow direction turned to follow the erosion of outer bank.

Preprints.org (www.preprints.org) | NOT PEER-REVIEWED | Posted: 3 February 2023 doi:10.20944/preprints202302.0064.v1

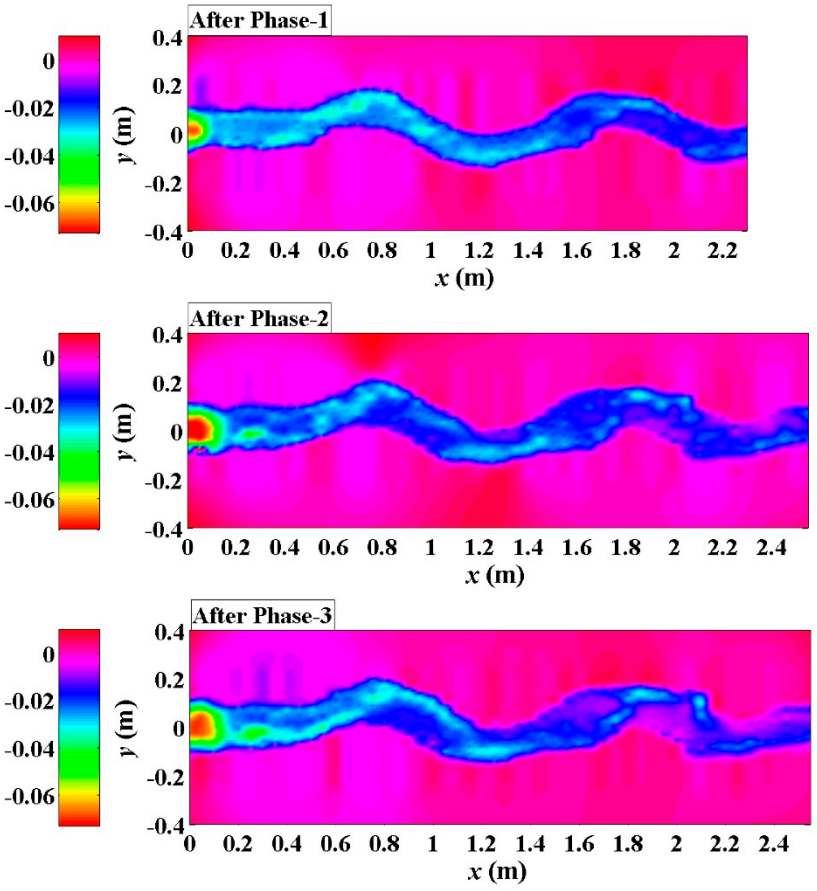

(a) Significant changes of DEMs (unit: m)

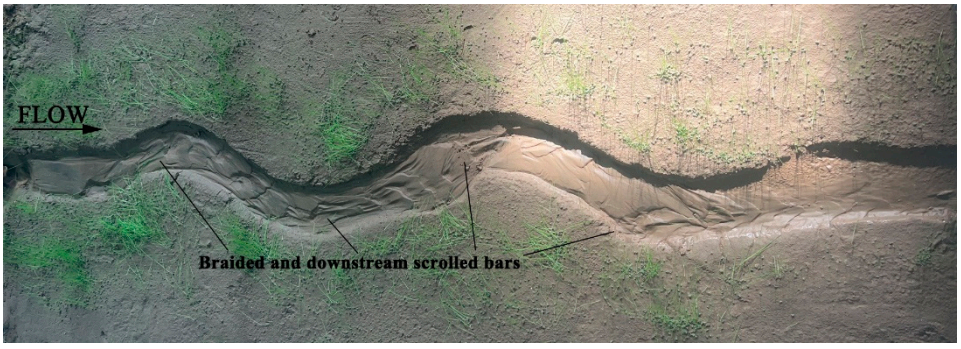

(b) Channel morphology after phase-1

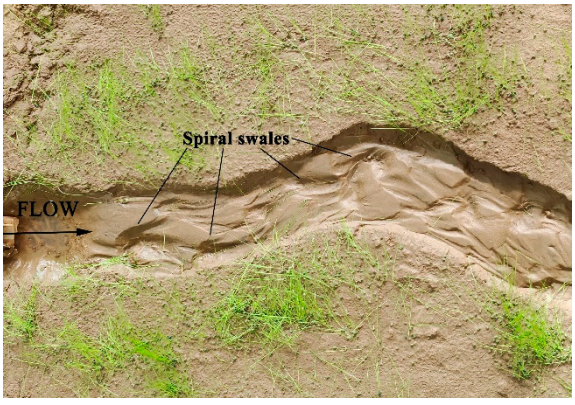

(c) Upstream bend morphology after phase-2

 doi:10.20944/preprints202302.0064.v1

(d) Transverse scrollbar morphology in phase-2

(e) Large-scale point-bar morphology after phase-3

Figure 6. Phased evolutions of the Lolium-perenne vegetation scenario (Run-c).

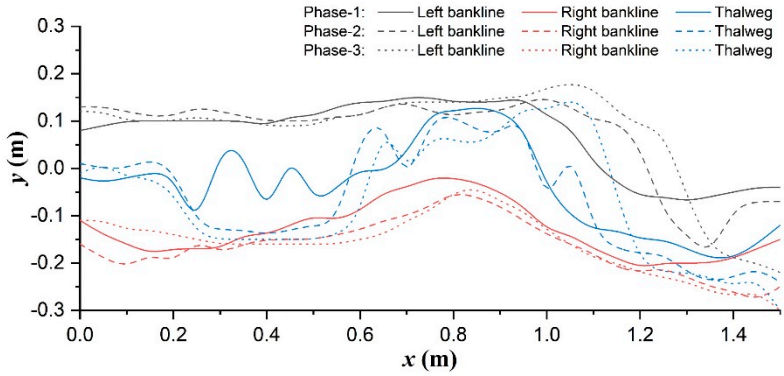

(a) Run-a

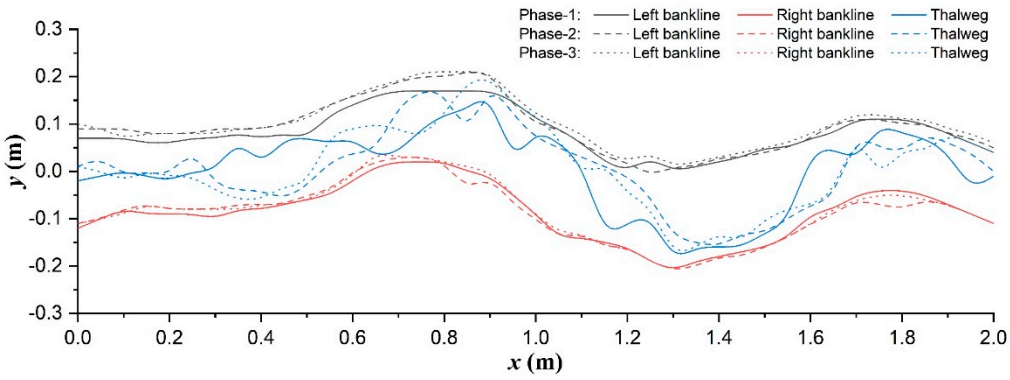

(b) Run-b

 doi:10.20944/preprints202302.0064.v1

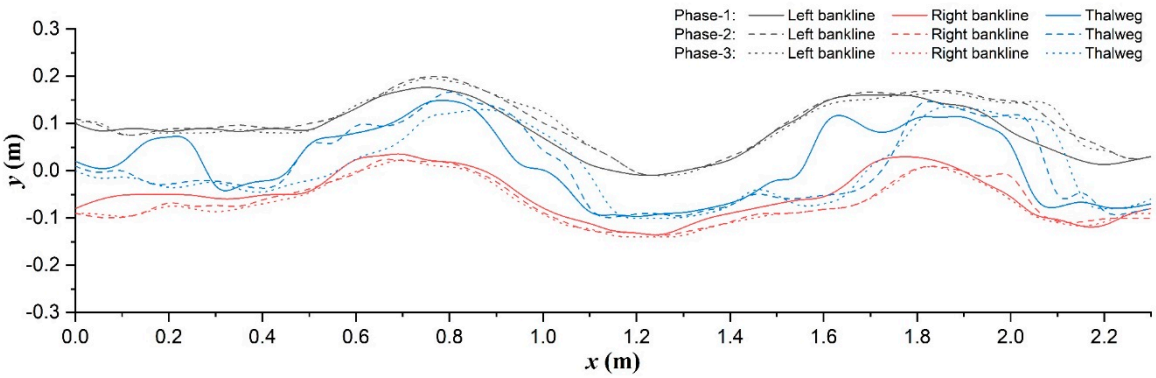

(c) Run-c

Figure 7. Bank-lines and thalweg migration of the main channel after three discharge phases in the (a) unvegetated scenario; (b) Festuca-elata vegetation scenario; and (c) Lolium-perenne vegetation scenario.

Significantly differently, in the Festuca-elata vegetation scenario (Figure 7b), the upstream channel was less widened (x<0.8m): both the outer and inner bank-lines clearly moved left, point bars accretion along the inner bank following the outer bank erosion can be confirmed in the No.1 bend under the driven of increasing discharge. Simultaneously, there occurred local inner-bank cutting corresponding to the bending apex of outer bank in both the No.1 bend (0.8m<x<0.9m) and No.3 bend (1.7m<x<1.9m) due to the deflecting flow disturbance of bare plant roots there, although the overall bank-lines seldom migrated after entering the No.2 bend and they basically would return to the preceding trace with slight widening after the falling back of discharge. In the Lolium-perenne vegetation scenario (Figure 7c), the channel belt widening was still restricted. The right-skewed migration of upstream straight segment was combined with the coupled inner-bank cutting and outer-bank erosion before and after each bend apex to happen in phase-2 in the overall meandering channel. Notably, there were not remarkable root disturbances like Run-b, but existed local vegetated bank failure around the inflection points of bends (x=1.0m, 2.1m) contributed by the decreasing discharge in phase-3.

Additionally, thalweg location was also altered by the bank vegetating. The thalweg of unvegetated floodplain was characterized with a lateral oscillation in upstream straight segment and the single-peak deviations towards outer-bank apex at each bend in phase-1 (Figure 7a); the latter pattern was changed to be double-peak deviations in the two vegetation scenarios, the former oscillation become weakening in Run-b (Figure 7a) and strengthening in Run-c (Figure 7c), respectively. Subsequently during the rising and falling processes of discharge, the upstream oscillating trend almost entirely vanished and was turned into the obvious right-skewness in all three scenarios, and especially, the deteriorating multi-peak deviation patterns were distinguished to occur at the No.1 bend in phase-2 in both Runs-a and c.

In simple terms, riparian vegetation promotes to weaken the upper vortex flow influences and to maintain the single-thread channel planform, in particular: deep-rooted plant helped to eliminate the lateral oscillation of thalweg and the inner-bank cutting effect originating from the upstream segment near the developing scour pit and greatly restrain the channel migration, but its bare roots would interfere the local flow structures obviously; however, shallow-rooted plant not only failed to eradicate the bank cutting, but actually flourished its long existence in the overall channel, which conformed to a meander straightening trend (Nagata et al., 2000) in the low width-depth-ratio experiments herein, and local vegetated outer-bank caving was also sharp resulted from the multi-peak distributed scour of flow as implied by thalweg forms.

3.2. Bed topography changes

Figure 8 shows the elevation profiles of thalweg along the longitudinal x-axis and streamwise s-axis in the three scenarios respectively. Figure 9 displays the graphical longitudinal coordinate

 doi:10.20944/preprints202302.0064.v1

transformations for assisting the observation and analysis. Compared with the general ascending trend in Run-a (Figure 8a) and descending trend in Run-c (Figure 8c), the thalweg elevation in the deep-rooted planting scenario maintained an average stability and gradually weakening fluctuation (Figure 8b). The smooth and stable curves can be observed in the near-inlet streamwise zone (0.1m<s<0.5m) in phase-1 in all three scenarios (right subfigures), but later they experienced significant changes in the opposite trends to their respective general along with the discharge changing (phases-2 and 3). The streamwise elevation profiles seldom show a quasi-regular topographic pattern related to ordinary alternate free bars even in these mature vegetation circumstances, which conflict with earlier findings of Kyuka et al. (2021) in simple

To consider erosion effects along the transverse axis perpendicular to thalweg, within the main flow channel, bed elevation data in terms of their position along and distance from the thalweg were interpreted through transformation between cartesian (x-y) and curvilinear orthogonal (s-n) coordinates (Merwade et al., 2005) and interpolation calculation (D'Errico, 2012a, 2012b, 2013). Figure 10 shows the phased changes of main channel bed elevation for all scenarios, especially, the comparisons of significant erosion locations in s-n coordinates. In both Runs-a and c, the largest scoured areas in the upstream flow path (s<0.5m) were observed to enlarge and shift positively (for n) as discharge increased, and to shrink and shift negatively (for n) as discharge decreased respectively; the largest scoured areas along the further flow path around the upstream No.1 bend apex in Run-a (0.75m<s<1.25m) and the upstream No.3 bend apex in Run-c (1.75m<s<2.25m) migrated downstream at their outer-bank sides and tended to be diminished at the diagonally opposite inner-bank sides respectively in phase-2; notably, such outer-bank scoured area was sensitive to discharge increase in Run-c and to discharge decrease in Run-a respectively, to become larger. In contrast, in Run-b, all the largest scoured areas around the near-inlet and near-bend regions turned to be weakened in phase-2; such typical area at the outer-bank side was located at similar flow locations to Run-c (around s=2.0m), yet was sensitive to discharge decrease to be more severely scoured like Run-a; moreover, such typical area at the inner-bank side migrated upstream in phase-3 instead (s=0.5~1.0m).

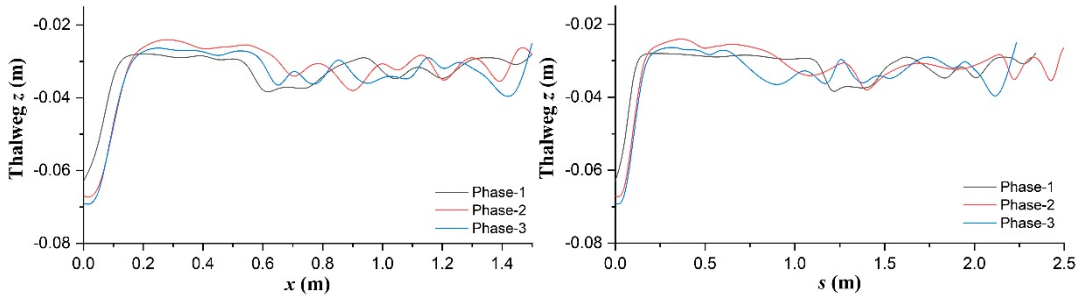

(a) Run-a

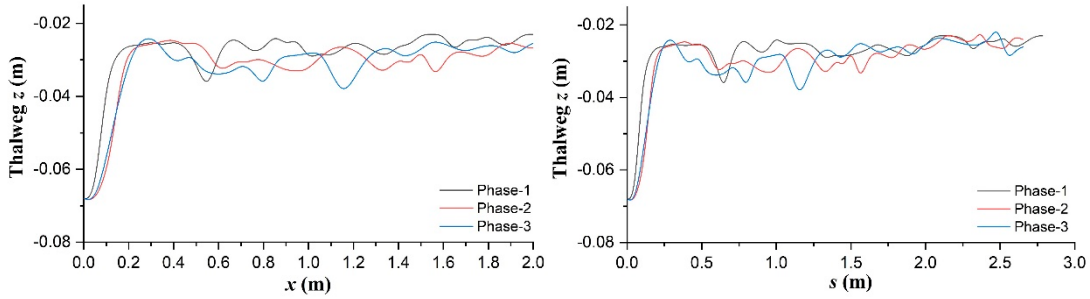

(b) Run-b

Preprints.org (www.preprints.org) | NOT PEER-REVIEWED | Posted: 3 February 2023 doi:10.20944/preprints202302.0064.v1

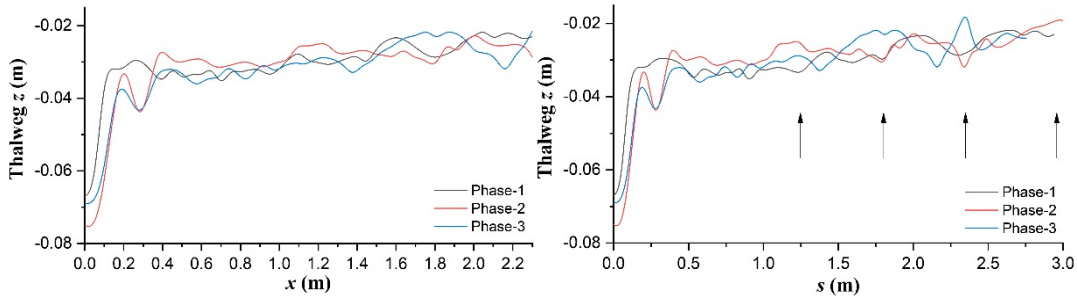

(c) Run-c

Figure 8. Thalweg elevation profiles along *x*-axis and *s*-axis respectively in the (a) unvegetated scenario; (b) Festuca-elata vegetation scenario; and (c) Lolium-perenne vegetation scenario.

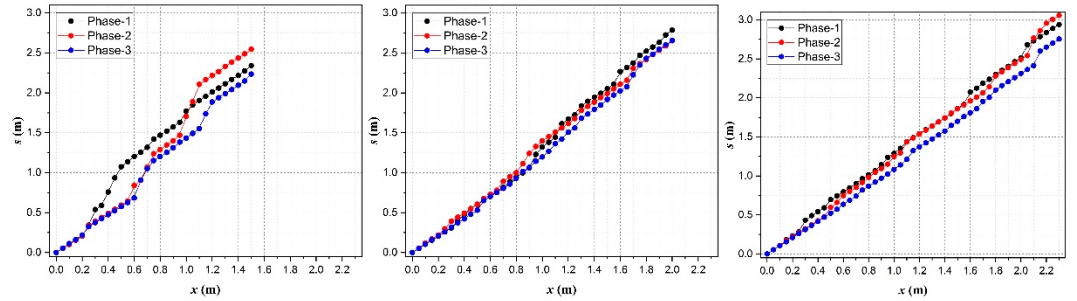

(a) Run-a (b) Run-b (c) Run-c

Figure 9. Transformation between *x* and *s* coordinates in various cases.

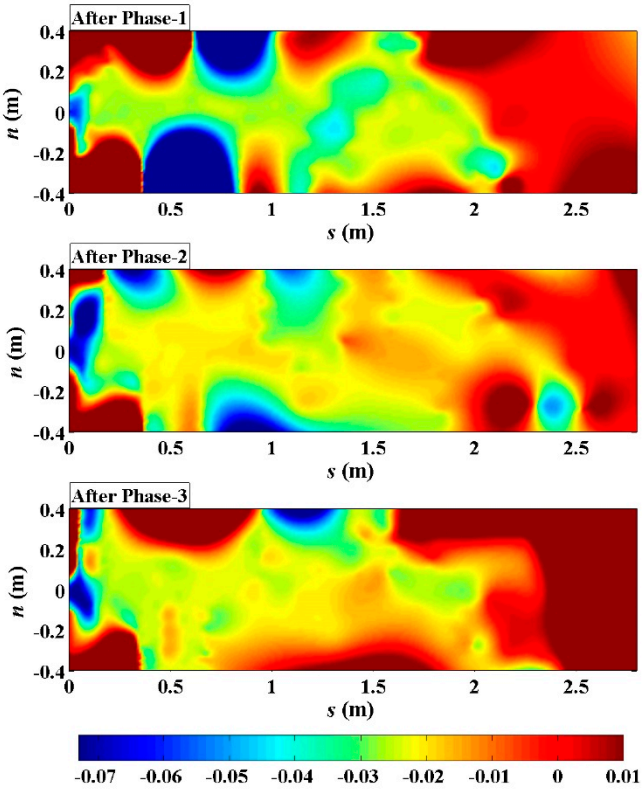

(a) Run-a

 doi:10.20944/preprints202302.0064.v1

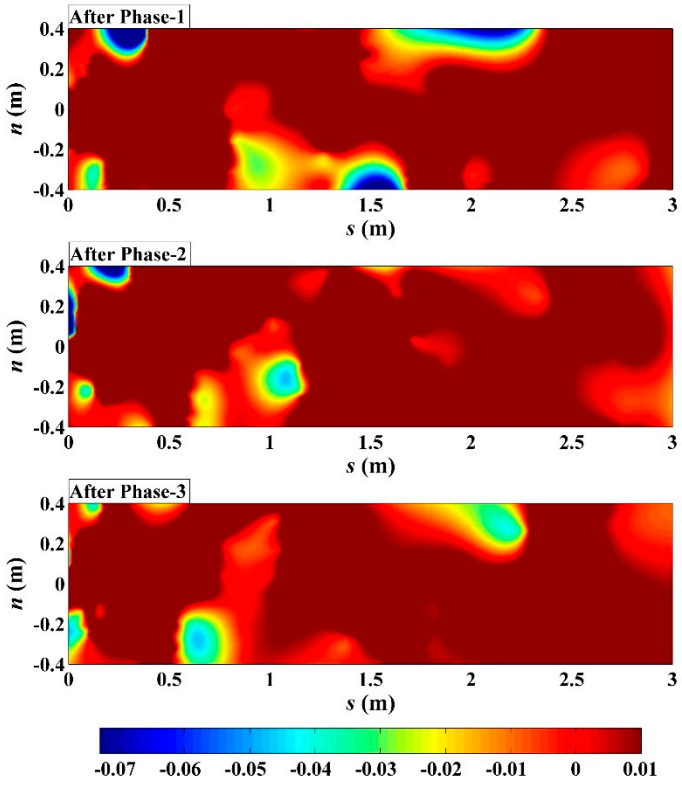

(b) Run-b

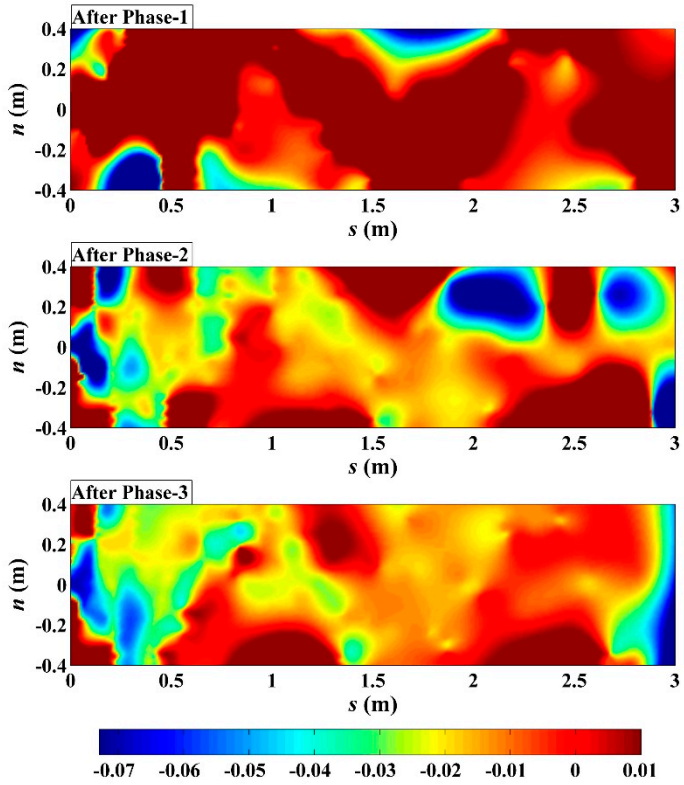

(c) Run-c

Figure 10. Phased changes of main channel bed elevation in the curvilinear orthogonal (*s*-*n*) coordinate system established based on thalweg in the (a) unvegetated scenario; (b) Festuca-elata vegetation scenario; and (c) Lolium-perenne vegetation scenario. The units are m.

 doi:10.20944/preprints202302.0064.v1

Evolutionary spectral analyses were performed to inspect typical changes in frequency patterns through the bed elevation data series along and distance from the thalweg (Figs. 11 and 12), based on the method of evolutionary fast Fourier Transform (FFT) (Kodama & Hinnov, 2014) in Acycle (Li et al., 2019). In terms of streamwise direction, in the unvegetated scenario (Figure 11a), multifrequency information were mainly concentrated in upstream straight segment (s<0.8m) in phase-1, then there occurred a jump of dominant frequency starting from the bifurcation interface of No.1 bend (s=1.4m) in phase-2, and higher multifrequency information long appeared in the middle and lower reaches even the fall back of discharge after phase-3. In the Festuca-elata vegetation scenario (Figure 11b), multifrequency information gradually spread further in No.2 bend (1.5m<s<2.0m) from the No.1 bend after the rising and falling of discharge and there weren't sharp frequency jumps in the course. In the Lolium-perenne vegetation scenario (Figure 11c), multifrequency information were mainly isolated in the interface between the upstream straight segment and No.1 bend (s=0.6m) and partly arose in the No. 3 bend (s>1.75m) as discharge decreased in phase-3.

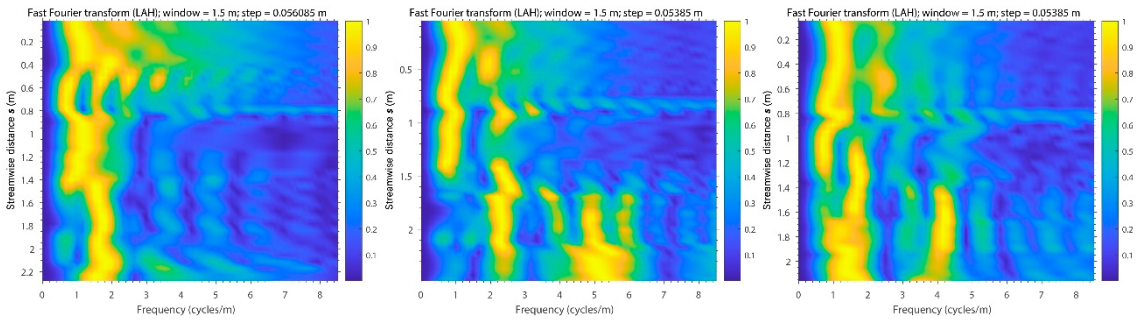

(a) Run-a

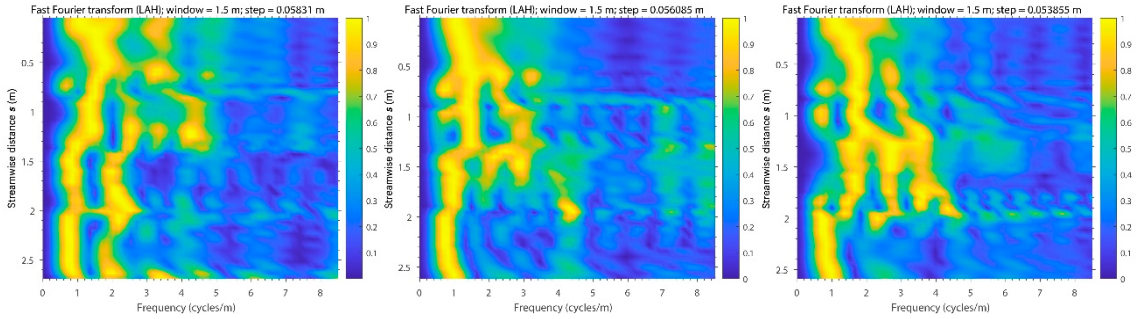

(b) Run-b

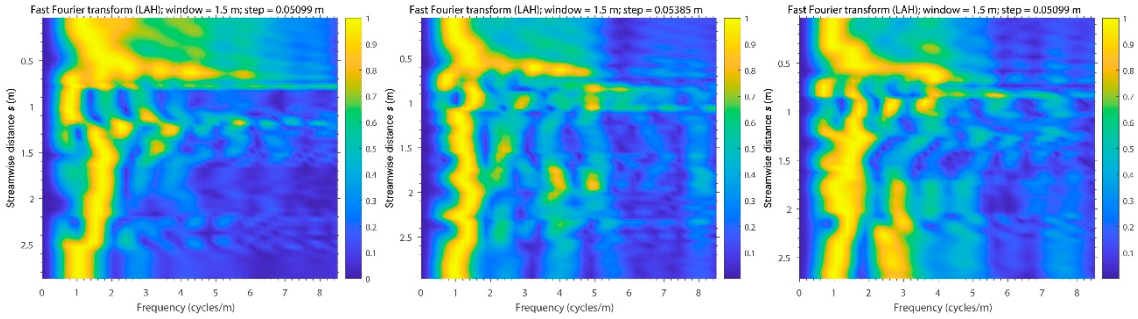

(c) Run-c

Figure 11. Evolutionary FFT through the thalweg elevation profiles along the streamwise direction in the (a) unvegetated scenario; (b) Festuca-elata vegetation scenario; and (c) Lolium-perenne vegetation scenario. (left: after phase-1; middle: after phase-2; right: after phase-3).

In typical transverse sections perpendicular to the thalweg with significant frequency changes as above:

Preprints.org (www.preprints.org) | NOT PEER-REVIEWED | Posted: 3 February 2023 doi:10.20944/preprints202302.0064.v1

Firstly, near the bifurcation interface of No.1 bend in Run-a (Figure 12a), there was already an obvious jump of information frequency at the location of *s*=1.4m in phase-1, the negative side here had continuous high frequency information, then the positive boundary zone (around *n*=0.4m) jumped high and an "entrainment effect" occurred near the graphical negative center (around *n*=-0.16m) as discharge increased in phase-2, and the entrainment disappeared when discharge decreased in phase-3. During the processes, relative to the stable upper section (*s*=1.3m), the lower section (*s*=1.5m) also went through such entrainment near the graphical negative center in phase-2, however, the positive side was gradually increasing along the positive direction and yet didn't reach the positive boundary in phase-3.

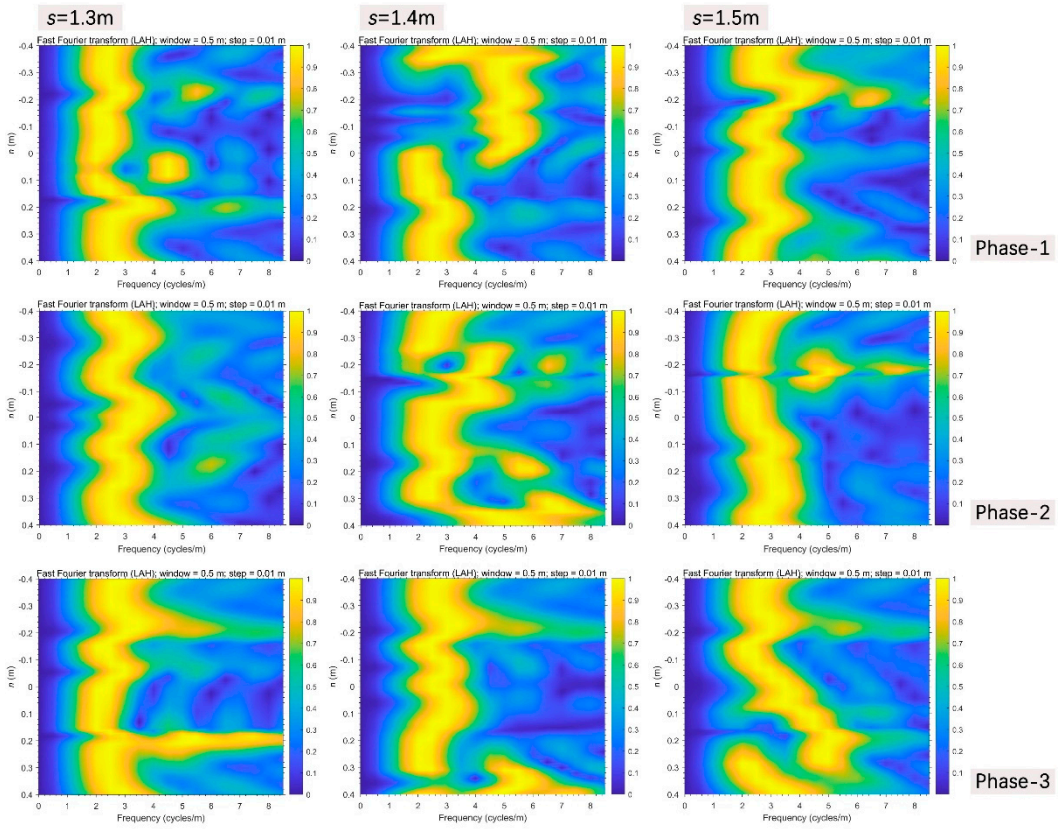

(a) Near the bifurcation interface of No.1 bend in Run-a

 doi:10.20944/preprints202302.0064.v1

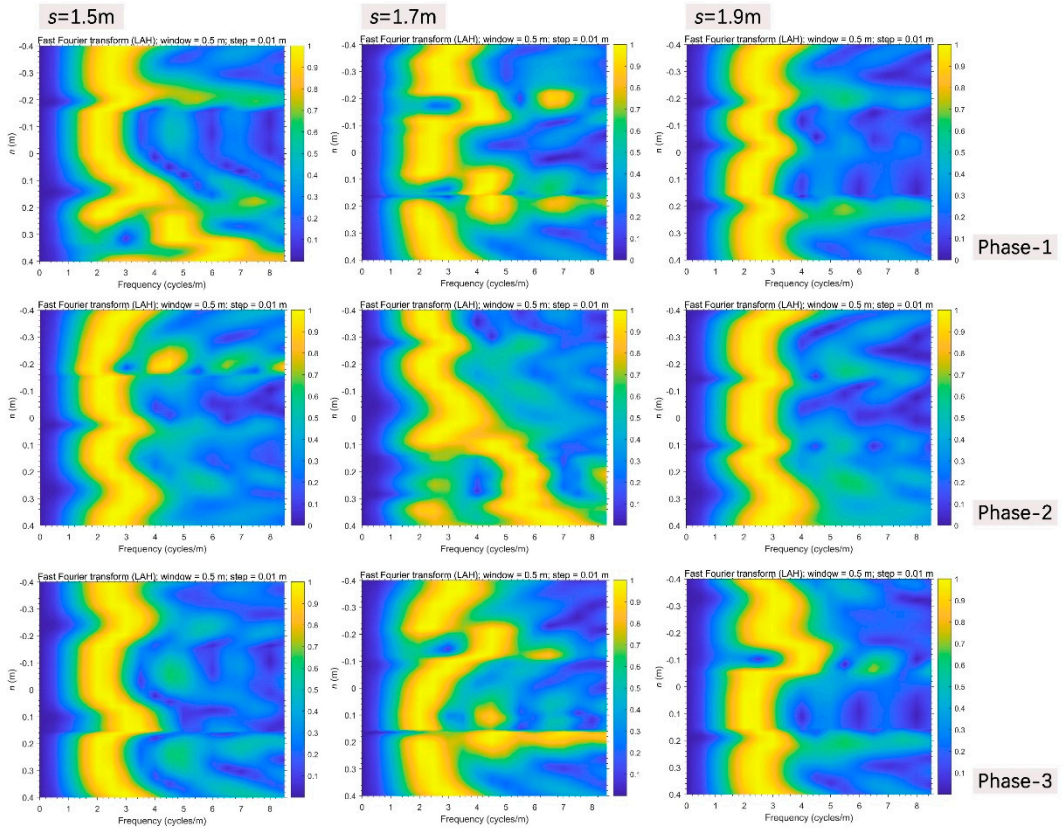

(b) Transition from No.1 bend to No.2 bend in Run-b

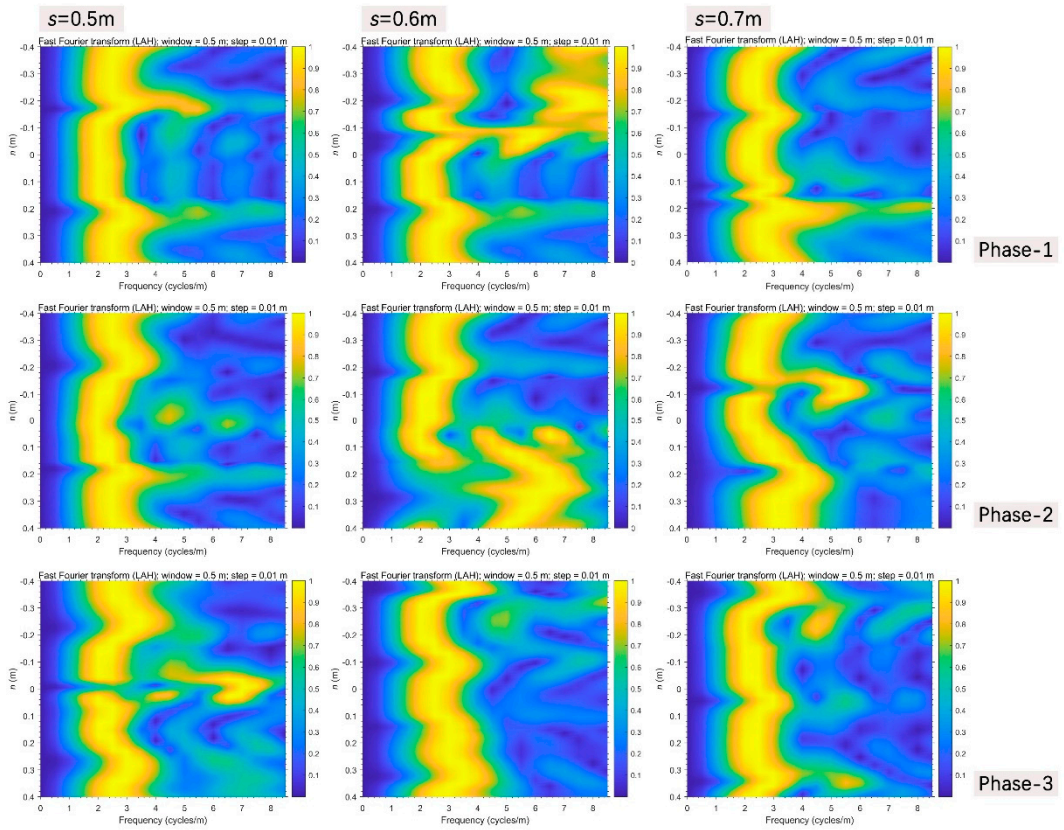

(c) Near the interface between upstream straight segment and No.1 bend in Run-c

Preprints.org (www.preprints.org) | NOT PEER-REVIEWED | Posted: 3 February 2023 doi:10.20944/preprints202302.0064.v1

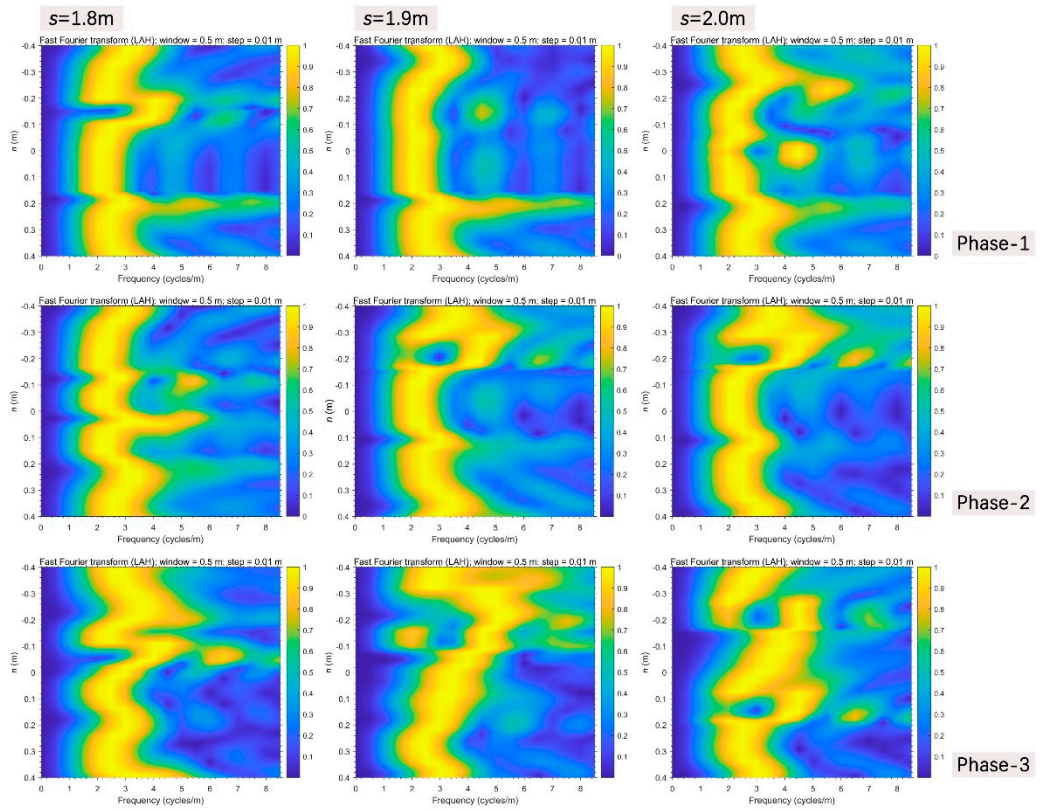

(d) No.3 bend in Run-c

Figure 12. Evolutionary FFT through the significantly changing transverse sections perpendicular to the thalweg in all three scenarios.

Secondly, in the No.2 bend in Run-b (Figure 12b), in phase-1, a gradual increase of information frequency along the positive direction clearly occurred in the positive side at the section of s=1.5m, and an entrainment happened in the graphical positive center (due to the diversion of inner-bank side) in the lower section of s=1.7m. Then in phase-2, the frequency distribution pattern of the upper section of s=1.5m was transferred downstream to the section of s=1.7m, yet the latter immediately returned to the previous state with the discharge decreasing in phase-3. The others always held stable forms.

Thirdly in Run-c, near the interface between the upstream straight segment and No.1 bend (Figure 12c), in phase-1, superhigh information frequency just occurred at the negative side of the critical section of s=0.6m, then they were completely transferred to the positive side when discharge increased, and finally come to peace after phase-3. In the upstream No.3 bend (Figure 12d), the enlargement of frequency information in phase-3 was highlighted at the negative boundary zone of the section of s=1.9m.

4. DISCUSSION

The geometry of a developed meandering channel is strongly related to the convective behavior of the vertically averaged initial flow over the flat bed, especially, the indicator of (maximum) deflection angle. The initial meandering channel in this experimental study can be classified as ingoing bend because of the deflection angle (35°) being falling near or below the lower critical values of 30° by da Silva (1995) and 50° by Tape (2001). Also, the flow patterns are a function of the width-depth ratio (W/d) of channel, in theory, our relatively narrow-deep experimental channel (W/d=6) would develop in accordance with meander straightening mode in temporal changes of planform (Nagata et al., 2000). However, a simple upper vortex flow driven by a dynamic growing scour pit was powerful enough to disturb the meandering channel flow structure and to affect meandering bank erosion and point-bar accretion. In the unvegetated scenario, lateral migration was centered

 doi:10.20944/preprints202302.0064.v1

around the nearest two bends to upper scour pit and point-bar development was replaced by downstream scrollbar evolution even after rising and falling of a flood. Braided swales in upstream bends clearly reflected the complex helical flow characteristics passed from the dynamic upper vortex flow. And hence the form of outer bank spray at the upstream bend was dendric instead of single-thread pattern in the face of flood. These are different from some traditional discussions (Kyuka et al., 2021; Leuven et al., 2018; van de Lageweg et al., 2014; van Dijk, van de Lageweg, et al., 2013) of meandering river.

Riparian vegetation coverage has been well understood to be able to play a key role in regulating morphodynamic evolution of a meandering channel and result in the transformation from a multi-thread to a single-thread channel planform by reducing fluvial erosion (Hopkinson & Wynn, 2009; Wynn & Mostaghimi, 2006) and geotechnical erosion (Pollen-Bankhead & Simon, 2010; Simon & Collison, 2002). And plant biodiversity (particularly the interactions between legumes and non-legumes) can reduce erosion rates indirectly through positive effects on root length and number of root tips (Allen et al., 2016). However, ecosystems contain not only multiple but various growth states of species that interact and coexist. Therefore, in the experimental saline-alkali soils, two common non-legume river landscape plants, i.e., Festuca-elata and Lolium-perenne, were adopted as the representative control vegetations to investigate the possible effects resulted from their nonuniform seedling normal growth. The characteristics of their unique root systems were demonstrated to dominate in the channel evolution variations with being less affected by environmental temperature and humidity (Table 1). In general, bank vegetating provided erosion resistance and prompted the narrowing of channel width and the concentration of flow into the main channel; and the vegetation almost took immediate effect on eradicating the occurrence of outward subsidiary channels during flood time, vegetation life stages seemed not be of significant influential as concluded by Kyuka et al. (2021), or rather, all the vegetated bank behaviors during the whole experimental processes could be viewed as being in mature stage; also, only the flood could bring on the point-bar development with transverse scroll ridges, for which the upper vortex flow disturbance clearly may need to be taken into consideration in the representative bank pull theory (van de Lageweg et al., 2014). Specifically, the shallow-rooted Lolium-perenne scenario was similar to the unvegetated scenario to yield to the falling process of discharge and was led to a deeper, narrower and meander developing (Nagata et al., 2000) main-channel; conversely, deep-rooted Festuca-elata merely created locally isolated flow disturbances as the long roots were continuously scoured and exposed within the main-channel, it perfectly maintained the few meander changes as indicated by the bank-lines and thalweg.

Usually in simple meandering channel, the inner-bank-line after outer-bank-line migrations were observed owing to firstly the erosion and retreat of outer banks and subsequently the sedimentation with new transverse scroll ridges along the inner banks (Pyrce & Ashmore, 2005). In our experiments, in comparison with initial meandering channel bank-line (Figure 1b), the unvegetated inner-bank line near the upstream scour pit was clearly cut and retreated more severe than the outer-bank line under the constant current scour, variation in the outer-bank line was primarily migration around the downstream half bend instead of erosion (Figure 7a); once passing the No.1 bend or vegetating banks, such local cutting effect of the upper vortex flow could be immediately reduced, the channel evolutions returned to the above common regular law; but shallow-rooted riparian vegetation still would yield to that effect when average discharge increased (Figure 7c), and the deep-rooted riparian vegetation might brought out the form of presentation of the shift of such vortex-flow effect to the downstream bends (Figure 7b) due to locally sparse vegetation cover (see Figure 5 for the riparian vegetation around the No.2 bend).

The thalweg marks the natural direction of a watercourse. Slowing channel bed erosion and protecting the erosion-deposit balance by taking advantage of a thalweg could help to stabilize running water sources and keep the ecosystem intact (Scheeler, 1990). Our experiments exhibited the imperishability of upper vortex-flow effects as it relatedly contributed to the lateral oscillation of unvegetated thalweg near the scour pit and the dispersedly sharpening of vegetated thalweg around the bend (Figure 7). Noteworthy was that only the deep-rooted vegetation could weaken the further complication of thalweg and stabilize the streamwise thalweg elevation (Figure 8), the transverse

 doi:10.20944/preprints202302.0064.v1

diffusion of flow energy along the thalweg was also the smallest here (Figure 10). Well, few studies focused on detailedly deconstructing the vertical bed changes in these circumstances so far relative to the meandering planform changes (Bolla Pittaluga et al., 2009; Camporeale et al., 2007; Crosato, 2008; Johannesson & Parker, 1989), for example in terms of a spectrum of frequencies or energies. Considering evolutionary spectral analysis was often used to estimate the power spectrum of a signal from its time-domain or depth-domain representation in geological research, we innovatively drew from this method to investigate the streamwise and transverse changes of frequency patterns of main-channel bed elevation in thalweg-based *s*-*n* coordinates, the overall results were quite different from channel centerline analysis on the common basis of assumption of constant discharge and ignorance of topography-driven lateral flow effect on longitudinal flow (Camporeale et al., 2007). Streamwise multifrequency information not only concentrated on the near vortex-flow generation zone, but when faced with a flood, also could be raised downstream the outward branching position, after experiencing the frequency uprush at *n*-positive boundary zone in combination with the frequency jump having existed at *n*-negative side on the critical transverse section in the unvegetated scenario; or spread along the roots disturbed main-channel with the shifting downstream of frequency distribution pattern of cutting-edge transverse section in the deep-rooted vegetation scenario; or changed to be highlighted in the turning interface of the upstream vortex-flow developing zone in the form of solitary high-frequency pillar distribution in the shallow-rooted vegetation scenario, in particular, the channel centerline analysis could be expected to be effective in the overall meandering channel here.

Nevertheless, the experimental scale is too small, various vegetation conditions are difficult to be accurately handled, the relationship between meandering channel morphodynamics and riparian vegetation under the circumstance of upper vortex-flow disturbances generated by a scour pit (e.g., waterfall or bridge pier) should be able to be better understood when combined with field-scale studies (Kui et al., 2014), and furtherly relevant numerical analysis need to address the effects of root networks carefully on vegetated-bank strengthening (Perona & Crouzy, 2018). Ecohydrology engineering approaches thereby will benefit from them much.

5. CONCLUSIONS

Our study highlights the crucial role of riparian vegetation in morphological processes of meandering river driven by the upper vortex flow from a scour pit. The following main findings are concluded: (1) downstream scrollbar evolution takes place of point-bar development in this complex channel condition, only the combination of vegetated-bank strengthening and flood scouring can bring on transverse point bars; (2) shallow-rooted vegetation is effective enough to regulate the channel to withstand flood scour to maintain the meander straightening mode of evolution (Nagata et al., 2000) without branching outward; (3) only deep-rooted vegetation can weaken the continuous inner-bank cutting originating from the upstream segment near the scour pit, but this resistant effect is susceptible to locally sparse coverage; (4) also, only deep-rooted vegetation can stabilize the thalweg and reduce the streamwise energy dispersion towards the surrounding environment; (5) evolutionary spectral analysis based on thalweg can reveal the streamwise variation of concentration of multifrequency information in vertical spaces, from the downstream region of bifurcation interface without vegetation, to the upstream local turning interface with shallow-rooted plant cultivating, then to the bare roots disturbed region with deep-rooted plant cultivating, and correspondingly, also can give transversely changing details in specific processes in orthogonal curvilinear coordinate system. These form a valuable basis for eco-engineering in river protection under the complex circumstances with the significant influence of upper vortex flow aroused by waterfall or bridge piers as examples.

Acknowledgements: This research is supported by the National Natural Science Foundation of China, Grant Nos. 51879182 and 51979185; the Open Research Fund of Key Laboratory of Hydro-Sediment Science and River Training, the Ministry of Water Resources, China Institute of Water Resources and Hydropower Research, Grant No. IWHR-JH-2020-A-02.

 doi:10.20944/preprints202302.0064.v1

References

Abernethy, B., & Rutherfurd, I. D. (2000). Does the weight of riparian trees destabilize riverbanks? *Regulated Rivers: Research & Management: An International Journal Devoted to River Research and Management, 16*(6), 565-576.

Allen, D. C., Cardinale, B. J., & Wynn-Thompson, T. (2016). Plant biodiversity effects in reducing fluvial erosion are limited to low species richness. *Ecology, 97*(1), 17-24.

Bertoldi, W., Siviglia, A., Tettamanti, S., Toffolon, M., Vetsch, D., & Francalanci, S. (2014). Modeling vegetation controls on fluvial morphological trajectories. *Geophysical Research Letters, 41*(20), 7167-7175.

Björk, C. R., Goward, T., & Spribille, T. (2009). New records and range extensions of rare lichens from waterfalls and sprayzones in inland British Columbia, Canada. *Evansia, 26*(4), 219-224.

Bolla Pittaluga, M., Nobile, G., & Seminara, G. (2009). A nonlinear model for river meandering. *Water Resources Research, 45*(4).

Bywater-Reyes, S., Diehl, R. M., & Wilcox, A. C. (2018). The influence of a vegetated bar on channel-bend flow dynamics. *Earth Surface Dynamics, 6*(2), 487-503.

Camporeale, C., Perona, P., Porporato, A., & Ridolfi, L. (2007). Hierarchy of models for meandering rivers and related morphodynamic processes. *Reviews of Geophysics, 45*(1).

Camporeale, C., Perucca, E., Ridolfi, L., & Gurnell, A. M. (2013). Modeling the interactions between river morphodynamics and riparian vegetation. *Reviews of Geophysics, 51*(3), 379-414.

Crosato, A. (2008). *Analysis and modelling of river meandering*: IOS press.

Crosato, A., & Saleh, M. S. (2011). Numerical study on the effects of floodplain vegetation on river planform style. *Earth Surface Processes and Landforms, 36*(6), 711-720.

D'Errico, J. (2012a). arclength (https://www.mathworks.com/matlabcentral/fileexchange/34871-arclength). *MATLAB Central File Exchange.* Retrieved Sep 27, 2022.

D'Errico, J. (2012b). interparc (https://www.mathworks.com/matlabcentral/fileexchange/34874-interparc). *MATLAB Central File Exchange.* Retrieved Sep 27, 2022.

D'Errico, J. (2013). distance2curve (https://www.mathworks.com/matlabcentral/fileexchange/34869-distance2curve). *MATLAB Central File Exchange.* Retrieved Sep 27, 2022.

da Silva, A. M. A. F. (1995). *Turbulent flow in sine-generated meandering channels*: Queen's University Kingston.

Gran, K. B., & Paola, C. (2001). Riparian vegetation controls on braided stream dynamics. *Water Resources Research, 37*(12), 3275-3283.

Gran, K. B., Tal, M., & Wartman, E. D. (2015). Co-evolution of riparian vegetation and channel dynamics in an aggrading braided river system, Mount Pinatubo, Philippines. *Earth Surface Processes and Landforms, 40*(8), 1101-1115.

Hopkinson, L., & Wynn, T. (2009). Vegetation impacts on near bank flow. *Ecohydrology: Ecosystems, Land and Water Process Interactions, Ecohydrogeomorphology, 2*(4), 404-418.

Jang, C.-L., & Shimizu, Y. (2007). Vegetation effects on the morphological behavior of alluvial channels. *Journal of Hydraulic Research, 45*(6), 763-772.

Johannesson, H., & Parker, G. (1989). Linear Theory of River Meanders. *River Meandering, AGU Water Resources Monograph (S. Ikeda and G. Parker, eds.)*, 181-214.

Kodama, K. P., & Hinnov, L. A. (2014). Time Series Analysis for Cyclostratigraphy. In *Rock Magnetic Cyclostratigraphy* (pp. 52-89).

Kui, L., Stella, J. C., Lightbody, A., & Wilcox, A. C. (2014). Ecogeomorphic feedbacks and flood loss of riparian tree seedlings in meandering channel experiments. *Water Resources Research, 50*(12), 9366-9384.

Kyuka, T., Yamaguchi, S., Inoue, Y., Arnez Ferrel, K. R., Kon, H., & Shimizu, Y. (2021). Morphodynamic effects of vegetation life stage on experimental meandering channels. *Earth Surface Processes and Landforms, 46*(7), 1225-1237.

Leuven, J. R., Braat, L., van Dijk, W. M., de Haas, T., Van Onselen, E., Ruessink, B., & Kleinhans, M. G. (2018). Growing forced bars determine nonideal estuary planform. *Journal of Geophysical Research: Earth Surface, 123*(11), 2971-2992.

Li, M., Hinnov, L., & Kump, L. (2019). Acycle: Time-series analysis software for paleoclimate research and education. *Computers & Geosciences, 127*, 12-22.

Lu, J., Li, Q., & Duo, L. (2002). Effect of salt stress on seed germination of Lolium perenne L. and Festuca elata Keng. *Bulletin of Botanical Research, 22*(3), 328-332. (in Chinese)

Merwade, V. M., Maidment, D. R., & Hodges, B. R. (2005). Geospatial representation of river channels. *Journal of Hydrologic Engineering, 10*(3), 243-251.

Nagata, N., Hosoda, T., & Muramoto, Y. (2000). Numerical Analysis of River Channel Processes with Bank Erosion. *Journal of Hydraulic Engineering, 126*(4), 243-252.

Parker, G., Shimizu, Y., Wilkerson, G., Eke, E. C., Abad, J. D., Lauer, J., . . . Voller, V. (2011). A new framework for modeling the migration of meandering rivers. *Earth Surface Processes and Landforms, 36*(1), 70-86.

Perona, P., & Crouzy, B. (2018). Resilience of riverbed vegetation to uprooting by flow. *Proceedings of the Royal Society A: Mathematical, Physical and Engineering Sciences, 474*(2211), 20170547.

Pollen-Bankhead, N., & Simon, A. (2010). Hydrologic and hydraulic effects of riparian root networks on streambank stability: Is mechanical root-reinforcement the whole story? *Geomorphology, 116*(3-4), 353-362.

Pyrce, R. S., & Ashmore, P. E. (2005). Bedload path length and point bar development in gravel-bed river models. *Sedimentology, 52*(4), 839-857.

Scheeler, C. A. (1990). *Umatilla River Basin, Anadromous Fish Habitat Enhancement Project: Annual Report 1989*.

Scheingross, J. S., & Lamb, M. P. (2017). A mechanistic model of waterfall plunge pool erosion into bedrock. *Journal of Geophysical Research: Earth Surface, 122*(11), 2079-2104.

Serlet, A. J., Gurnell, A. M., Zolezzi, G., Wharton, G., Belleudy, P., & Jourdain, C. (2018). Biomorphodynamics of alternate bars in a channelized, regulated river: An integrated historical and modelling analysis. *Earth Surface Processes and Landforms, 43*(9), 1739-1756.

Simon, A., & Collison, A. J. (2002). Quantifying the mechanical and hydrologic effects of riparian vegetation on streambank stability. *Earth Surface Processes and Landforms, 27*(5), 527-546.

Song, X., & Bai, Y. (2015). A new empirical river pattern discriminant method based on flow resistance characteristics. *Catena, 135*, 163-172.

Song, X., Bai, Y., & Ying, C. (2014). A three-dimensional topographic survey based on two-dimensional image information. *Journal of Zhejiang University SCIENCE A, 15*(1), 68-82.

Song, X., Xu, G., Bai, Y., & Xu, D. (2016). Experiments on the short-term development of sine-generated meandering rivers. *Journal of Hydro-environment Research, 11*, 42-58.

Song, X., Xu, H., & Bai, Y. (2022). The systematic out-branching (Dragon style) rivers under the perspective of connection between river morphology and ecology. *Ecohydrology & Hydrobiology, 22*(3), 505-510.

Tal, M., & Paola, C. (2007). Dynamic single-thread channels maintained by the interaction of flow and vegetation. *Geology, 35*(4), 347-350.

Tape, W. (2001). *Experimental investigation of flow patterns in meandering channels of moderate sinuosity*. University of Windsor, Canada.

Terwilliger, V. J. (1990). Effects of vegetation on soil slippage by pore pressure modification. *Earth Surface Processes and Landforms, 15*(6), 553-570.

van de Lageweg, W. I., Van Dijk, W. M., Baar, A. W., Rutten, J., & Kleinhans, M. G. (2014). Bank pull or bar push: What drives scroll-bar formation in meandering rivers? *Geology, 42*(4), 319-322.

van Dijk, W. M., Teske, R., van de Lageweg, W. I., & Kleinhans, M. G. (2013). Effects of vegetation distribution on experimental river channel dynamics. *Water Resources Research, 49*(11), 7558-7574.

van Dijk, W. M., van de Lageweg, W. I., & Kleinhans, M. G. (2013). Formation of a cohesive floodplain in a dynamic experimental meandering river. *Earth Surface Processes and Landforms, 38*(13), 1550-1565.

Vargas-Luna, A., Crosato, A., Calvani, G., & Uijttewaal, W. S. (2016). Representing plants as rigid cylinders in experiments and models. *Advances in water resources, 93*, 205-222.

Wynn, T., & Mostaghimi, S. (2006). The effects of vegetation and soil type on streambank erosion, southwestern virginia, usa 1. *JAWRA Journal of the American Water Resources Association, 42*(1), 69-82.

Yang, S., Bai, Y., & Xu, H. (2018). Experimental Analysis of River Evolution with Riparian Vegetation. *Water, 10*(11), 1500.

Zalewski, M. (2013). Ecohydrology: process-oriented thinking towards sustainable river basins. *Ecohydrology & Hydrobiology, 13*(2), 97-103.

Zalewski, M. (2015). Ecohydrology and hydrologic engineering: regulation of hydrology-biota interactions for sustainability. *Journal of Hydrologic Engineering, 20*(1), A4014012.